

Dynamic Species Interactions in the San Nicolas Island Kelp Forest

Empirical dynamic modeling analysis

Owen Liu

March 13, 2018

Introduction

This document accompanies the manuscript “...” The following analyses lay out the building blocks of the empirical dynamic modeling approach (Ethan R. Deyle et al. 2016; Chang, Ushio, and Hsieh 2017) that produced the final version of the analyses in the paper.

In the analysis that follows, in each step that involves a new type of EDM method, its logic will be briefly described. However, keep in mind that the basic theory behind each individual method is the same: We use some dynamic information (from single or multiple time series) to reconstruct a shadow attractor, and then use the properties of that manifold to make predictions.

1. Variables in the Data

The San Nicolas Island Dataset

San Nicolas Island is a small, remote island situated about 100 kilometers offshore from southern California. The island itself is small, about 14 kilometer long and 5 km wide. The data in the analysis is from a sampling station on the western end of San Nicolas Island. The benthic monitoring data herein have been collected more or less every six months for more than 35 years by the USGS and its Western Ecological Research Center (USGS-WERC), and in 2013 the datasets were made available publicly through Ecological Archives:

Michael C. Kenner, James A. Estes, M. Tim Tinker, James L. Bodkin, Robert K. Cowen, Christopher Harrold, Brian B. Hatfield, Mark Novak, Andrew Rassweiler, and Daniel C. Reed. 2013. A multi-decade time series of kelp forest community structure at San Nicolas Island, California (USA). *Ecology* 94:2654. <http://dx.doi.org/10.1890/13-0561.1>

And in 2016, the data were again compiled and an updated version was published online:

Miller R., A. Rassweiler, D. Reed, K. Lafferty, L. Kui, M. O'Brien. 2016. Santa Barbara Channel Marine BON: Integrated quad and swath cover. Environmental Data Initiative.

Physical Oceanographic Data

A body of other research has established that a combination of physical forcing (waves, storms), temperature, and lower frequency climate modes (e.g., El Niños) have an important influence on the dynamics of kelp forests (Reed et al. 2011; Cavanaugh et al. 2011; Bell et al. 2015, Young et al. (2015)). With these data, we can draw connections between the physical variables and the species interactions in our constrained trophic web.

We have four datasets, already processed into the same time frame (periods) as the SNI benthic monitoring data:

- **The Multivariate ENSO index (MEI)**
 - The first principal component of a composite set of physical parameters

- Positive values of the MEI index are generally associated with El Nino conditions, decreases in wind-driven upwelling, warmer surface waters and nutrient-poor conditions
- Variable here is the average index value for the four months preceding each Spring or Fall monitoring period (i.e., December to March or June to September, respectively)
- **The Pacific Decadal Oscillation index (PDO)**
 - Leading empirical orthogonal function (EOF) of monthly sea surface temperature anomalies (SST-A) over the North Pacific (poleward of 20° N) after the global average sea surface temperature has been removed
 - Positive PDO values indicate warmer SST, and nutrient-poor conditions along the western coast of the contiguous United States
 - Aggregated and averaged the same way as MEI
- **The North Pacific Gyre Oscillation (NPGO)**
 - From (Di Lorenzo et al. 2008)
 - Climate pattern that emerges as the 2nd dominant mode of sea surface height variability (2nd EOF SSH) in the Northeast Pacific
 - Better correlated with salinity, nutrients, and chlorophyll than PDO, showing forcing for the planktonic community
 - Strong predictor of upwelling cells south of 38 deg N
 - Aggregated and averaged the same way as MEI and PDO
- **Sea surface temperature (SST)**
 - Two sources (to fill in data gaps):
 - Sea surface temperature data directly from Begg Rock and San Nicolas Island buoys, from the Coastal Data Information Program (CDIP)
 - NOAA's Optimally Interpolated Sea Surface Temperature
 - Similar to the above, value is an average SST for the four months preceding each period
- **Maximum significant wave height (Hs)**
 - Combined data from the Begg and SNI buoys with modeled data from the Geophysical Fluid Dynamics Laboratory
 - Significant wave height is defined as the average height, in meters, of the one third highest waves in the record
 - Instead of an average, value here is the maximum significant wave height of the four months preceding each period. This is meant to capture any large storm events, as well as general level of physical disturbance

Unlike the biological data, where there are unique spatial replicates, the physical data have only one value for each of the 69 monitoring periods, and hence their values are replicated (copied) for each site to match the total length of the biological data.

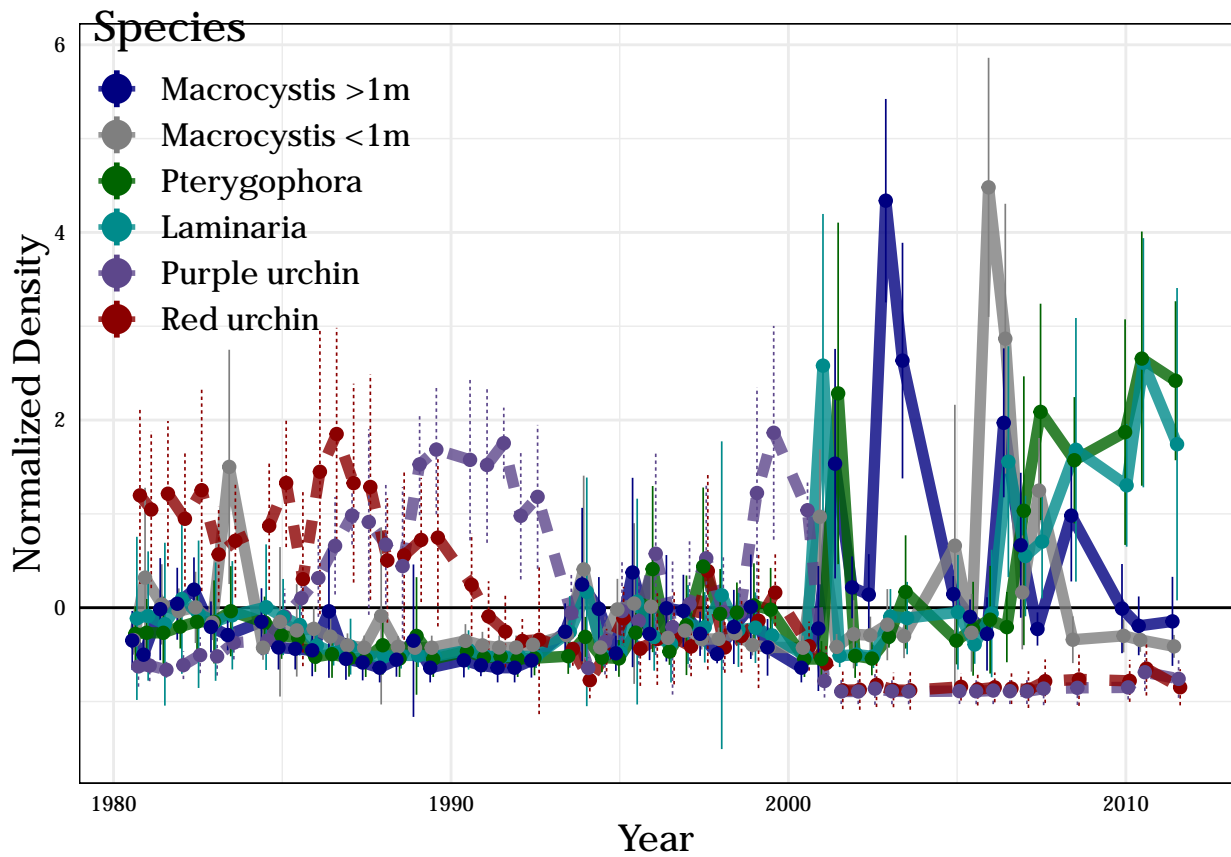
Note about data processing

Usual best practice for EDM is to create normalized time series, so that state-space reconstructions are not distorted by differences in orders of magnitude between variables. In addition, in this study we concatenate each species/station/swath time series into one long time series for each species, while preserving a time indicator (variable ‘period’) and a site identifier, to ensure that we do not “cross” the boundaries of replicate time series in analyses. Empirical dynamic modeling can use multiple spatial replicates in lieu of increased length of individual time series, to maximize the dynamic information that can be drawn from the system (C.-h. Hsieh, Anderson, and Sugihara 2008; Clark et al. 2015; Chang, Ushio, and Hsieh 2017).

All raw data is available online or in the included files. We join the monitoring and physical datasets and normalized all time series (see scripts in the “data” folder for details:

Variable	Description
site	Monitoring Transect
period	Monitoring Period

Variable	Description
lam	Laminaria Normalized Density
mac	Macrocystis pyrifera >1m Normalized Density
pter	Pterygophora Normalized Density
purp	Strongylocentrotus purpuratus Normalized Density
red	Mesocentrotus franciscanus Normalized Density
ymac	Macrocystis pyrifera <1m Normalized Density
mei	Normalized Multivariate ENSO Index
pdo	Normalized Pacific Decadal Oscillation
npgo	Normalized North Pacific Gyre Oscillation
waves	Normalized Maximum Significant Wave Height
sst	Normalized Sea Surface Temperature



2. Establishing Univariate Predictability and Nonlinearity

For each of these time series, we have a few steps to see if they seem appropriate to analyze together with EDM techniques (Chang, Ushio, and Hsieh 2017). We want to be careful that our state space reconstructions are reliable and represent valid manifolds. In other words, we don't want to rely on simple cross-correlation or the prior knowledge that all these data were collected around the same locations at around the same times. We want evidence that:

1. Variables can be probably embedded (i.e., they show evidence of limited system dimensionality)

- Variables display state-dependent (nonlinear) dynamics, and therefore that nonlinear (EDM) methods are appropriate for analysis of these data

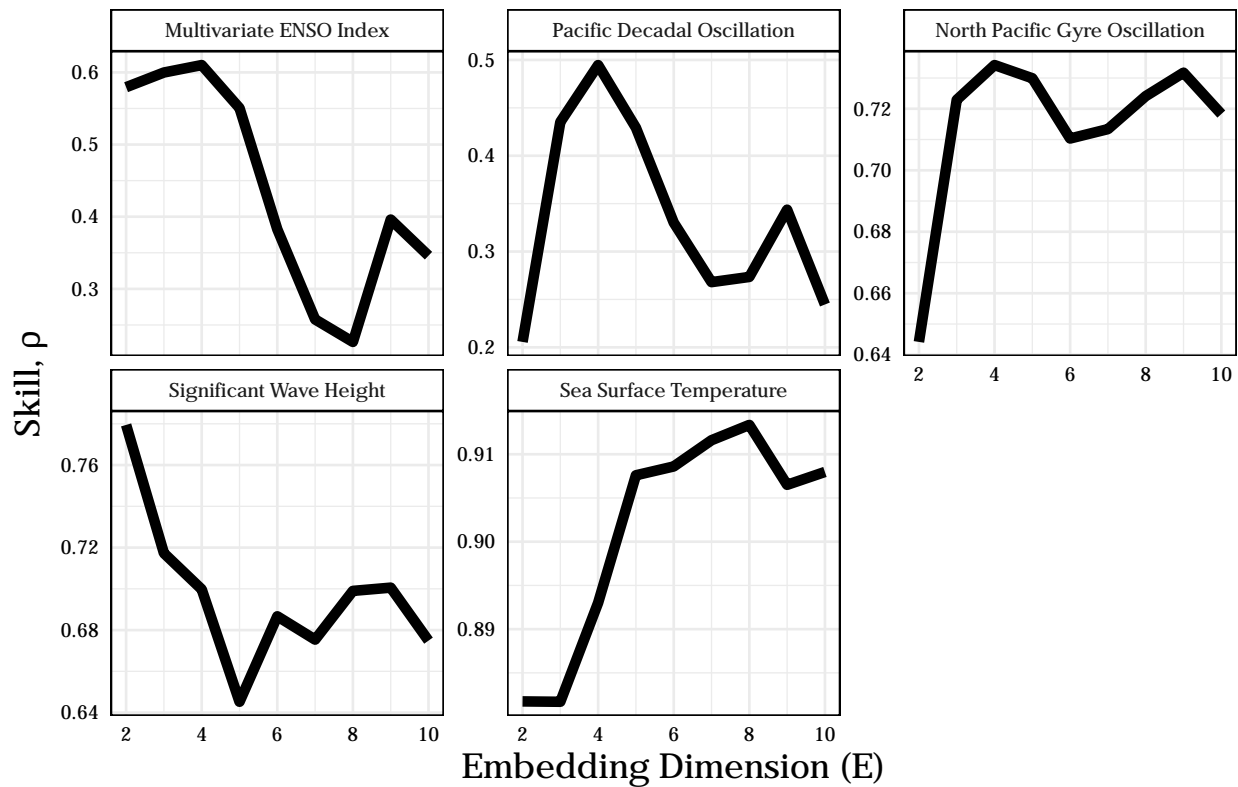
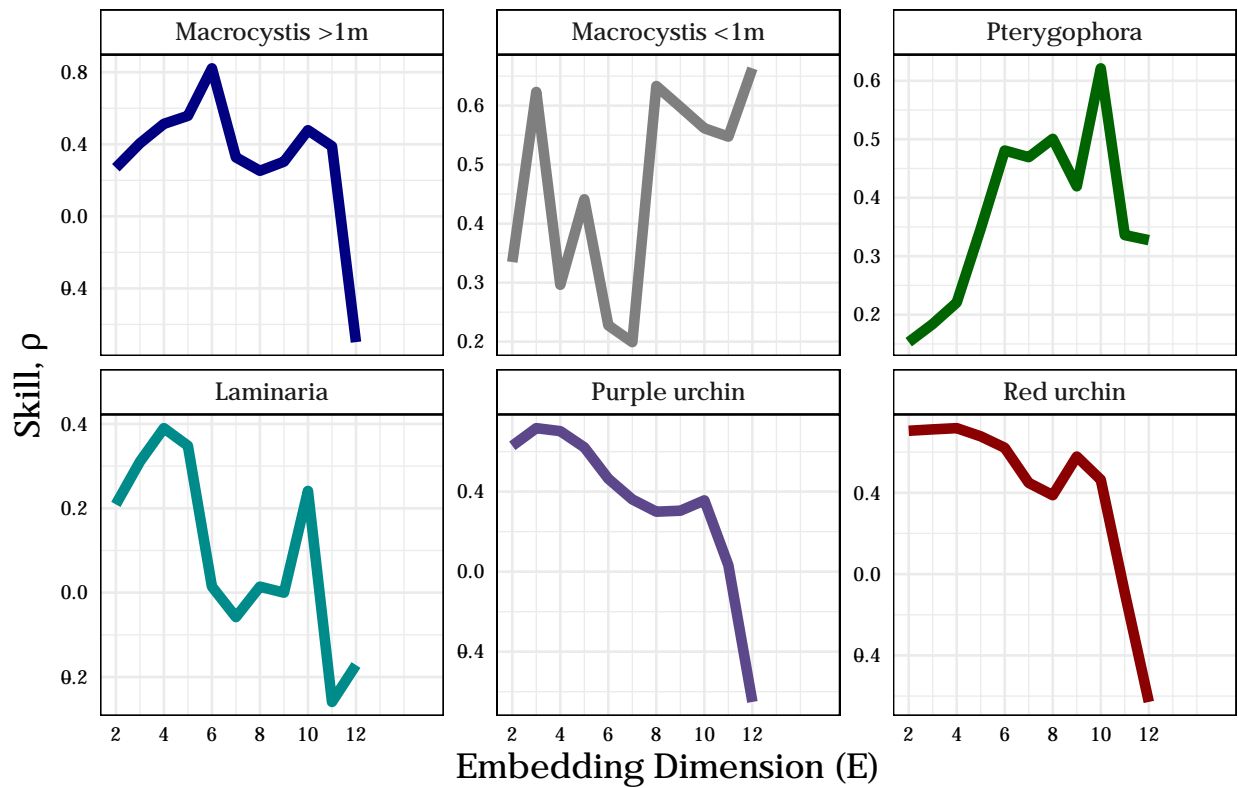
First, we use simplex projection to get a sense of system dimensionality for each variable, which will also give us an idea of the appropriate embedding dimension to use in later analyses. Then, we explicitly look for evidence of state-dependence and nonlinear dynamics with a prediction horizon test and S-maps.

Simplex Projection and Embedding Dimensions

For each species/variable separately, we will search for signals of deterministic behavior using simplex projection. In simplex projection, we first reconstruct a shadow attractor in E dimensions, where E is the number of variables, or number of progressive lags of a single variable used in the reconstruction. E is called the ***embedding dimension***. The E -length vectors, for example $\mathbf{x}_t = \langle x_t, x_{t-1}, x_{t-2} \rangle$ are points on the attractor, and the set of E -length vectors used for the reconstruction is called the ***library***. To predict \mathbf{x}_{t+1} , the simplex algorithm finds the $E + 1$ nearest neighbors of \mathbf{x}_t in the state space, and the prediction $\hat{\mathbf{x}}_{t+1}$ is the average of the nearest neighbors' values at $t + 1$, weighted by their Euclidean distance from \mathbf{x}_t at t . This is the essence of simplex projection: a forecast for a given point in state space is surmised from the forward trajectories of observed nearby points.

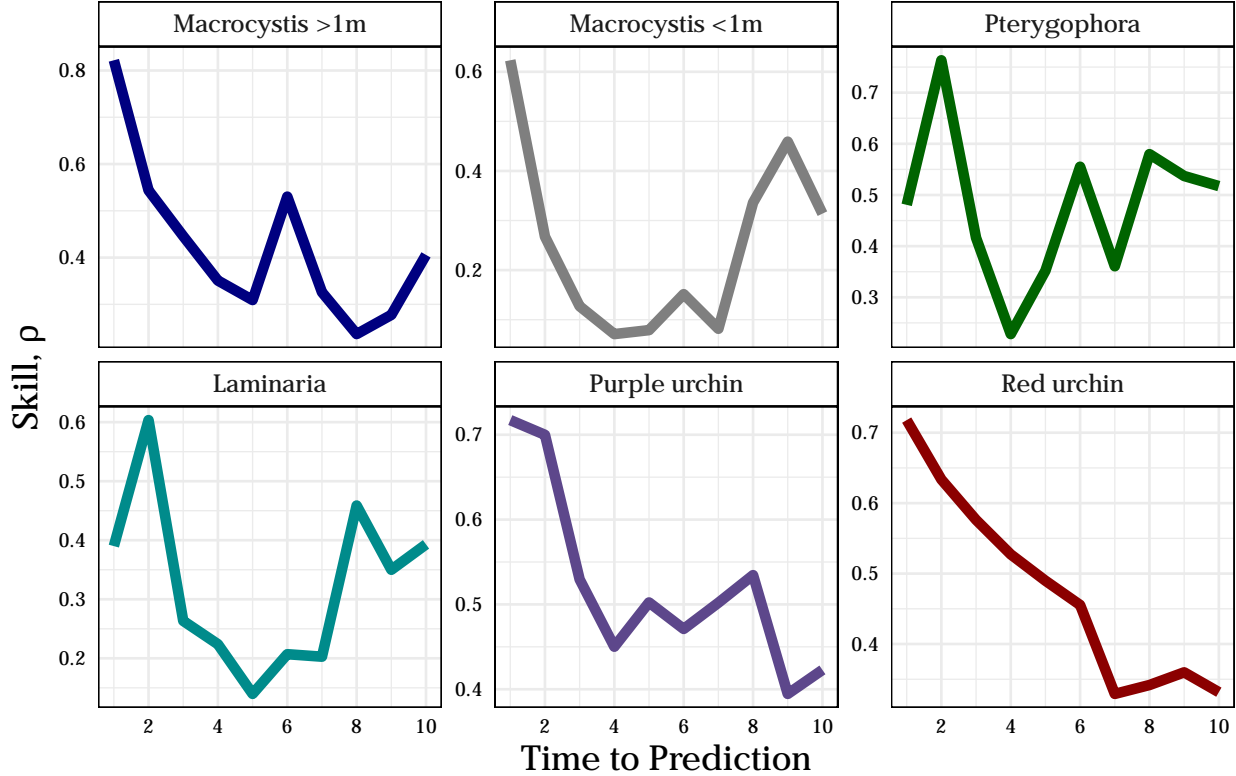
In descriptive terms, this is akin to asking, “When the system has been in a state like this before, what happened next?” For example, if we are interested in predicting *Macrocystis* density next year, we might take the current three-year density trend (this year, last year, and the year before, $E=3$) and compare it to a subset of times in the past when successive three-year dynamics looked similar to that set of points. Our prediction, logically, would be the average of that subset, projected forward one year and weighted by their similarity to the current trend.

By varying the value of E , we can determine what the best embedding dimension is for each variable in our analysis, essentially a proxy for the number of variables that best “unfolds” or best represents the shadow attractor. We can measure the skill of an embedding by comparing the estimated forecasts $\hat{\mathbf{x}}_{t+1}$ with the observed values \mathbf{x}_{t+1} , and we report it with ρ , the Pearson correlation coefficient between predictions and observations. To avoid in-sample fitting, we use a leave-one-out cross-validation scheme, removing one vector at a time from the library, and predicting its dynamics from the other library vectors.



Prediction Horizon test

We also want to look at prediction decay for each variable, which is one piece of evidence that a dynamic system is nonlinear. Using the best E identified in the previous step, we attempt to make predictions increasing far into the future, instead of just one period ahead. A nonlinear system should show decreasing predictive power with increasing prediction horizon (Sugihara 1994). This phenomenon is a property of deterministic chaos and is analogous to the “butterfly effect”, where in a nonlinear system, trajectories in state-space are expected to diverge over time. To examine this effect, we hold E constant, and proceed with simplex projection as before, but varying the prediction horizon, t_p (i.e., how many steps ahead we try to predict).



The prediction horizon effect check is promising overall, as most variables decline in predictive ability with increasing time horizon. For *Pterygophora californica*, *Macrocystis* juveniles, and *Laminaria*, there is some evidence of cyclic behavior, in that dynamics are more predictable 6 periods in the future than 3 or 4 periods.

S-maps for Each Species

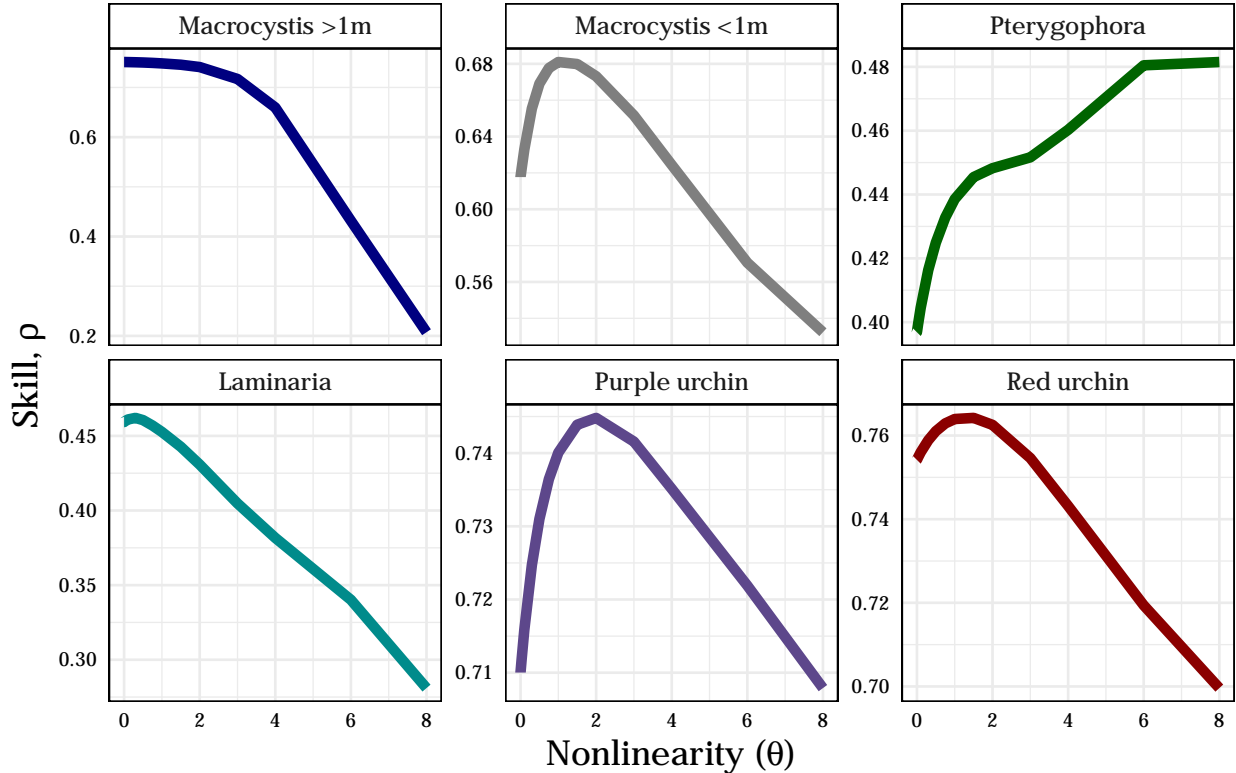
All of the variables show a decent ability to self-predict, as shown by simplex projection, although some variables require rather high embedding dimensions, indicative of higher-dimensionality dynamics. However, the butterfly effect check is evidence of potential nonlinearity, as all variables decline in predictive ability with time horizon.

We can look for further evidence of nonlinearity with S-maps. S-maps is short for “sequentially weighted global linear maps”, and it is similar to simplex projection, except instead of using just the $E+1$ nearest neighbors to make forecasts, S-maps uses all library vectors, and exponentially weights them by their distance to the prediction vector before using linear regression to make a forecast. A parameter, θ , tunes how much greater weight is given to nearby points. If $\theta = 0$, all library vectors are weighted equally, and the resulting

model is just a vector autoregressive (VAR) model of order E . However, as θ is tuned above 0, nearby points in state-space are given more weight in forecasts. Therefore, if model skill ρ increases with increasing θ , it is evidence of nonlinear, state-dependent dynamics. For a more formal description of the S-maps procedure, see Sugihara (1994) and Ethan R. Deyle et al. (2016).

As a side note, with $\theta > 0$, although the set library vectors remains constant, the *weights* given to library vectors for regression is specific to each point in state-space, and therefore a separate linear map is created for each predicted vector. This is why the procedure is called “sequentially weighted global linear maps”. Conceptually, as the dynamic system moves along the surface of the attractor, S-maps sequentially computes linear maps to the next point based on nearby points.

For prediction of each variable using S-maps, we can again use the optimal embedding dimension, E , found through our simplex projection above, and we plot the tuning parameter θ against ρ to look for evidence of nonlinear dynamics.



All variables show significantly improved predictive ability with increased theta, suggesting nonlinear dynamics. Together, the simplex, prediction horizon, and S-map results suggest our approach is valid—variables are predictable, and most predictable in a nonlinear manner.

3. Convergent Cross Mapping

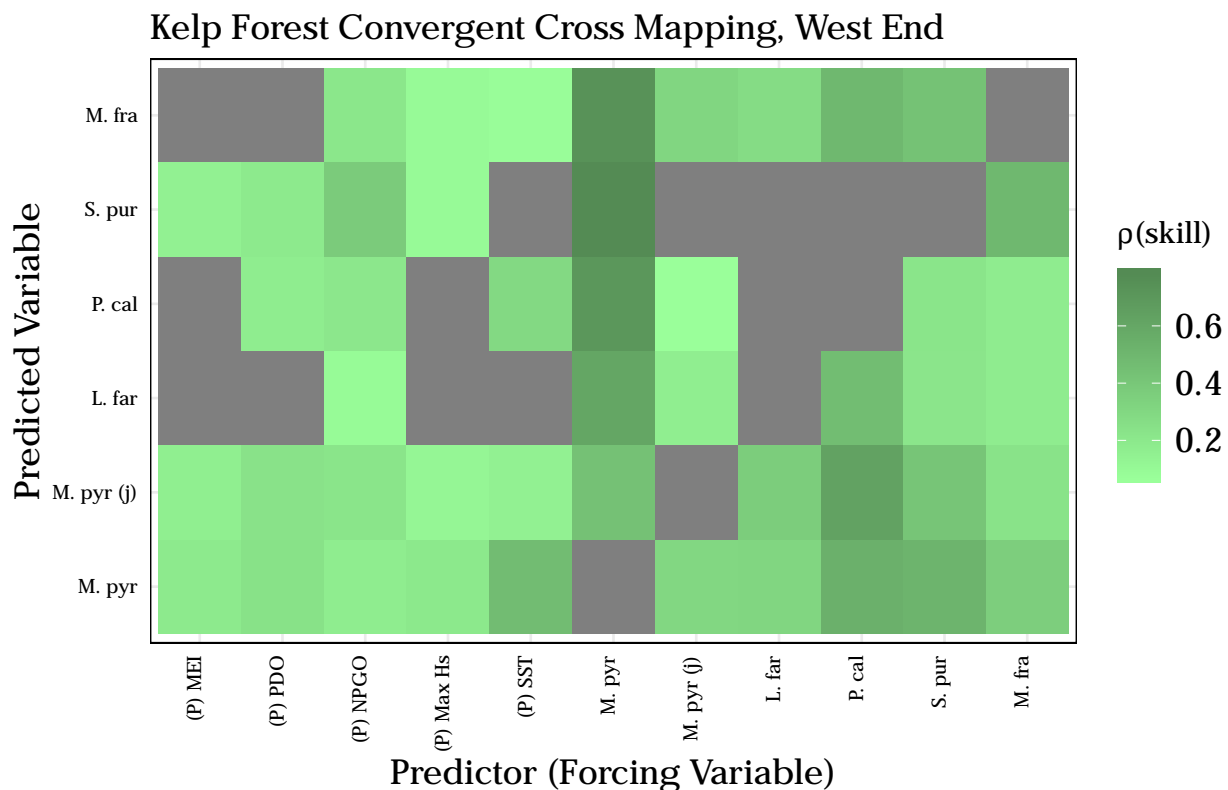
Generalizations of Takens' theorem indicate that if two variables (in our case, species or physical variables) are part of the same dynamic system, their individual dynamics should reflect their relative causal influence (Sugihara et al. 2012; Ethan R Deyle et al. 2013, Ye et al. (2015), Clark et al. (2015)). In other words, if one variable (for example, giant kelp), is causally forced by another (sea urchins), that forcing should leave a signature on the giant kelp time series. Convergent cross mapping (CCM) tests for causation by using the attractor/manifold built from the time series of one variable to predict another. CCM works

just like univariate simplex projection that we did in Step 1, except that separate variables are used for library and prediction vectors. In addition, we normally predict contemporaneous values of the other variable, instead of projecting one step forward (prediction horizon $t_p = 0$). If the attractor can accurately (based on out-of-sample prediction skill, just as before) predict the dynamics of the second variable, we can claim that the second variable has a causal influence on the first. In other words, the *causal effect of A on B is determined by how well B cross-maps A*. In this way, the inference from cross-mapping is the converse direction of causation. In our example, if sea urchins drive giant kelp, the dynamic information from the urchin time series should be reflected in the kelp dynamics, and kelp should significantly cross-map the urchins.

Cross-mapping can distinguish unidirectional forcing (A forces B but B does not force A) from bi-directional (A and B force each other). It can also resolve transitive causal chains (A causes B causes C, see Fig. 4 in Sugihara et al. (2012)). To look for a causal signal, we plot predictive skill ρ against library size (the number of embedded vectors used to construct the attractor). There are two criteria for CCM to establish causality: * First, and most obviously, predictive cross-map skill using all available data should be significantly greater than zero. * Second, that predictability should be convergent. Convergence means that cross-mapped estimates improve with library length, because the attractor is more fully resolved and therefore estimation error should decline. Convergence is key to distinguishing causation from simple correlation.

The CCM algorithm uses a random sampling method to test multiple “versions” of each library size, sampling a subset from the supplied library vectors to give a sense of the confidence intervals around prediction skill. We again use leave-one-out cross-validation to prevent in-sample fitting.

We can use CCM theory to ensure that the species in our data are actually displaying causal signals.



The plot shows cross-mapped (predictor, or forcing) variables in the columns, while rows are predicted variables. Gray indicates a lack of significant causal signal, and darker colors represent higher cross-map skill.

From this plot, we can make a few observations. The five physical forcing variables are represented in the first five columns, followed by the algae and urchin species. Many physical variables show causal relationships

with kelp forest species, especially the North Pacific Gyre Oscillation and Pacific Decadal Oscillation, which show causal links to almost all the biological variables. The NPGO is cross-mapped well by the purple urchin *Strongylocentrotus purpuratus*, while SST in turn shows a strong influence on adult *Macrocystis* dynamics. So already we are seeing effects that we might expect based on known interactions between physical variables and biological dynamics (Reed et al. 2011; Bell et al. 2015).

Additionally, adult *Macrocystis* itself seems to be a strong driver of the dynamics of many, if not all the other species in the trophic web, supporting the decades of research showing the importance of giant kelp as a foundational species (Graham, Vásquez, and Buschmann 2007; Dayton 1985), but further suggesting that its dynamics fundamentally drive the dynamics of other species. Juvenile, or sporophyte *Macrocystis*, on the other hand, is affected by most of the variables in the system, but does not itself drive dynamics of other species, again an effect we would expect to find. In this system, *Pterygophora californica* also seems to be a significant driver of the dynamics of other species in the trophic web.

Both sea urchin species are causal predictors of *Macrocystis* density, and they also have a causal effect on one another. This analysis alone, however, does not yet tell us whether the bi-directional interaction between *S. purpuratus* and *M. franciscanus* represents apparent mutualism, apparent competition, or a mixture of both at different times. To further investigate the direction and magnitude of the species interactions themselves, we next build multivariate EDM models that explicitly measure dynamic species interaction strengths.

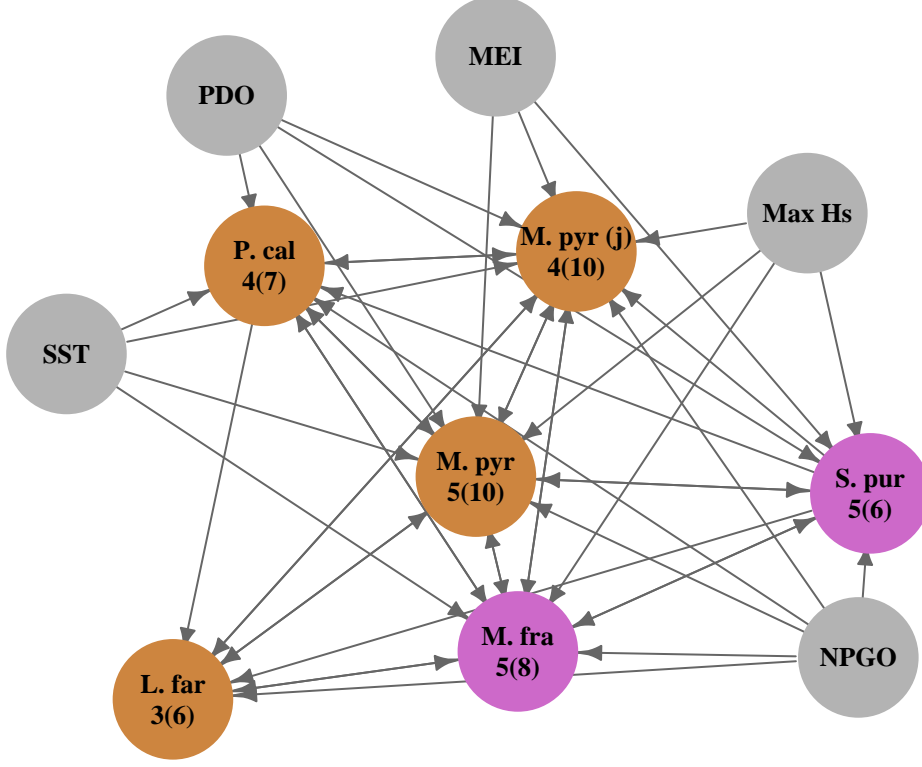
4. Multivariate Models Using CCM results

Every EDM method we have used so far involves reconstructing an attractor in state-space and then examining that attractor to make predictions. In Step 2, we used single time series and their lags to build attractors, and examined the attractors for evidence of the degree of dimensionality, predictability, and nonlinearity. In Step 3, we built attractors from one species and searched for the signature of other species' dynamics encoded in those attractors, leading to inferences about causation.

Multivariate models have the same structure, except instead of using single variables to reconstruct the attractors, we use contemporaneous values of multiple variables (Ethan R. Deyle et al. 2016). Instead of library vectors or points in state-space taking the form of, for example, $\langle x_t, x_{t-1}, x_{t-2} \rangle$, they now are formed in true multivariate space, e.g. $\langle Kelp_t, Urchin_t, Nutrients_t \rangle$. Using the normalized time series, we will build library vectors that each include the variable we are trying to predict, as well as other causal variables illuminated by our CCM analysis. Then we use S-maps as above to forecast the target variable using leave-one-out cross-validation just as in Step 3.

Interaction Network

The CCM results translated into an empirical interaction web looks like this:



In this network, each node represents a variable, and the numbers associated with each are the number of causal connections in the web, outgoing and (incoming). The maximum number of outgoing interactions is 5 (6 total biological variables minus the variable itself), and incoming is 10 (5 biological and 5 physical variables). Algae species are in brown, while the two urchin species are in purple and the physical drivers are in grey. For example, as mentioned above, we can see that young *Macrocystis* (denoted *M. pyr (j)*) is forced by all other variables in the system, but only itself shows a causal forcing on 4 of the 5 other biological variables. Again we can see that while the web is not entirely saturated, there are many unidirectional forcings, and a prevalence of bidirectional causation as well (A forces B *and* B forces A). The adult *Macrocystis* is causally connected to all variables in the analysis.

Dynamic Species Interaction Models

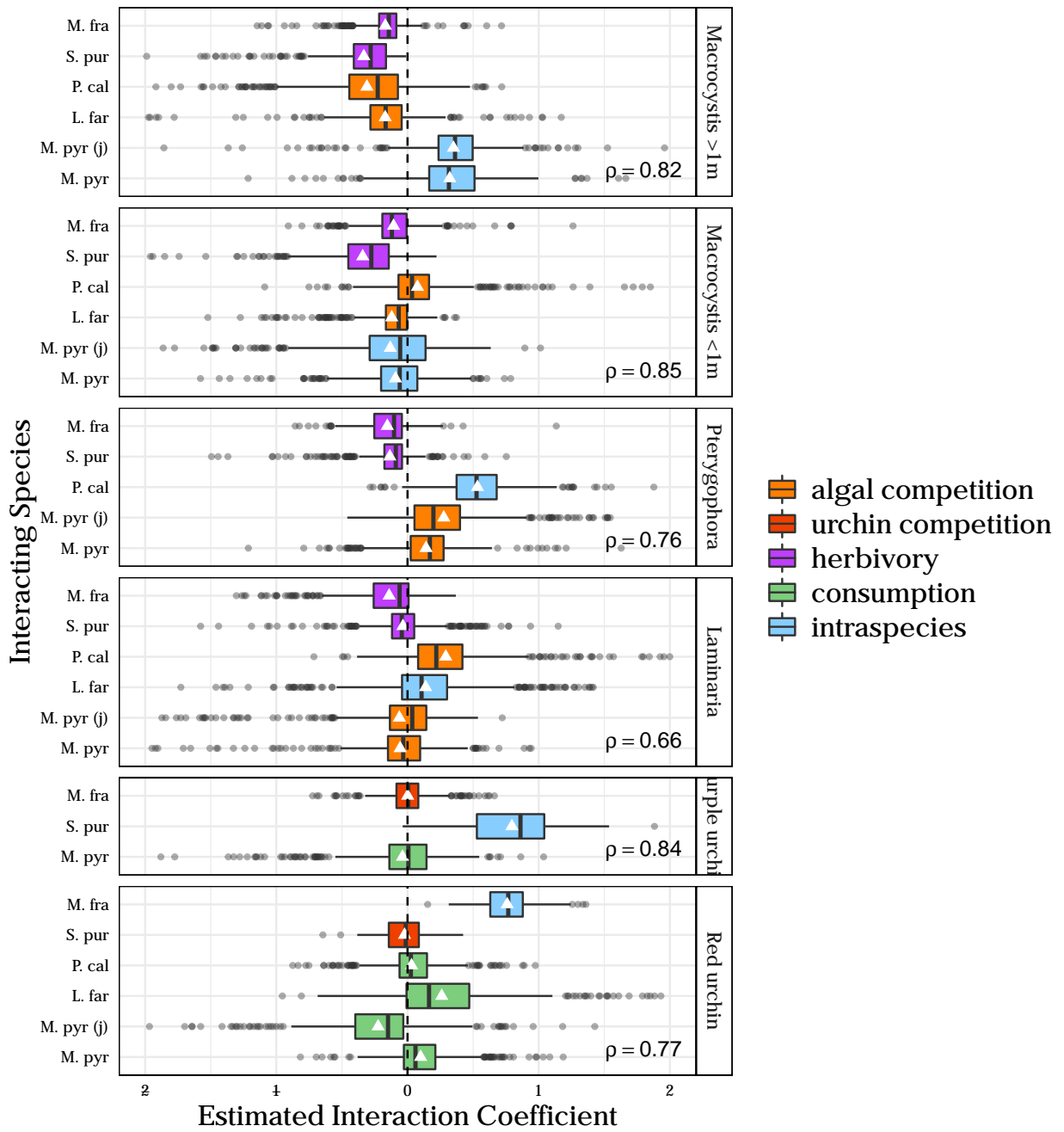
When we construct multivariate models for the six variables in the data based on their causal relationships, we get multivariate S-map models that perform well, displaying a high level of correlation between out-of-sample predictions and observed values, and relatively low mean absolute error (MAE).

Modeled Species	Predictors	ρ	MAE
Macrocystis	Laminaria, Pterygophora, Purple urchin, Red urchin, Macrocystis <1m, Multivariate ENSO Index, Pacific Decadal Oscillation, North Pacific Gyre Oscillation, Significant Wave Height, Sea Surface Temperature, Macrocystis >1m	0.825	0.370
Purple Urchin	Macrocystis >1m, Red urchin, Multivariate ENSO Index, Pacific Decadal Oscillation, North Pacific Gyre Oscillation, Significant Wave Height, Purple urchin	0.845	0.349
Laminaria	Macrocystis >1m, Pterygophora, Purple urchin, Red urchin, Macrocystis <1m, North Pacific Gyre Oscillation, Laminaria	0.663	0.379
Young Macrocystis	Laminaria, Macrocystis >1m, Pterygophora, Purple urchin, Red urchin, Multivariate ENSO Index, Pacific Decadal Oscillation, North Pacific Gyre Oscillation, Significant Wave Height, Sea Surface Temperature, Macrocystis <1m	0.852	0.332
Red Urchin	Laminaria, Macrocystis >1m, Pterygophora, Purple urchin, Macrocystis <1m, North Pacific Gyre Oscillation, Significant Wave Height, Sea Surface Temperature, Red urchin	0.774	0.381
Pterygophora	Macrocystis >1m, Purple urchin, Red urchin, Macrocystis <1m, Pacific Decadal Oscillation, North Pacific Gyre Oscillation, Sea Surface Temperature, Pterygophora	0.763	0.334

5. Results

Multivariate Model Output: Species interactions

We can pull from the models every predicted interaction between species. These fitted interaction strengths are specifically the estimated effect of the density of one species on itself or another species, when forecasting one monitoring period (approximately six months) ahead. For example, each data point for *Pterygophora* in the *Macrocystis* model is the predicted effect of the current density of Pterygophora on the density of Macrocystis in the next monitoring period. Mathematically, each interaction measured is a partial derivative, or element of our sequentially calculated Jacobian matrices, estimating the effect of one species on another, $\delta N_1 / \delta N_2$. The distributions of those interactions are shown in the figure below.



These are box-and-whisker plots of estimated species interaction strengths from S-map models for the five focal species (panels top to bottom): *Macrocystis* adults, *Macrocystis* juveniles, *Pterygophora*, *Laminaria*, purple urchin, and red urchin. Each colored box represents the distribution of all estimated interaction coefficients (x-axis) of an interacting or forcing species (left y-axis) on a modeled species (right y-axis) across all data for a given model (vertical lines: median; box: interquartile range; whiskers extend to data point at most $1.5 * IQR$ from the box). Correlation coefficient between predictions and observations denoted for each model. Color denotes hypothesized interaction type, including interspecific competition (between algae species or between urchin species), herbivory (urchin effect on algae), consumption (algae effect on urchins), and intraspecies interaction (the estimated interaction of a species with itself). Abbreviations: *S. pur*, *Strongylocentrotus purpuratus*; *P. cal.*, *Pterygophora californica*; *M. pyr*, *Macrocystis pyrifera*; *M. fra*, *Mesocentrotus franciscanus*; *L. far*, *Laminaria farlowii*.

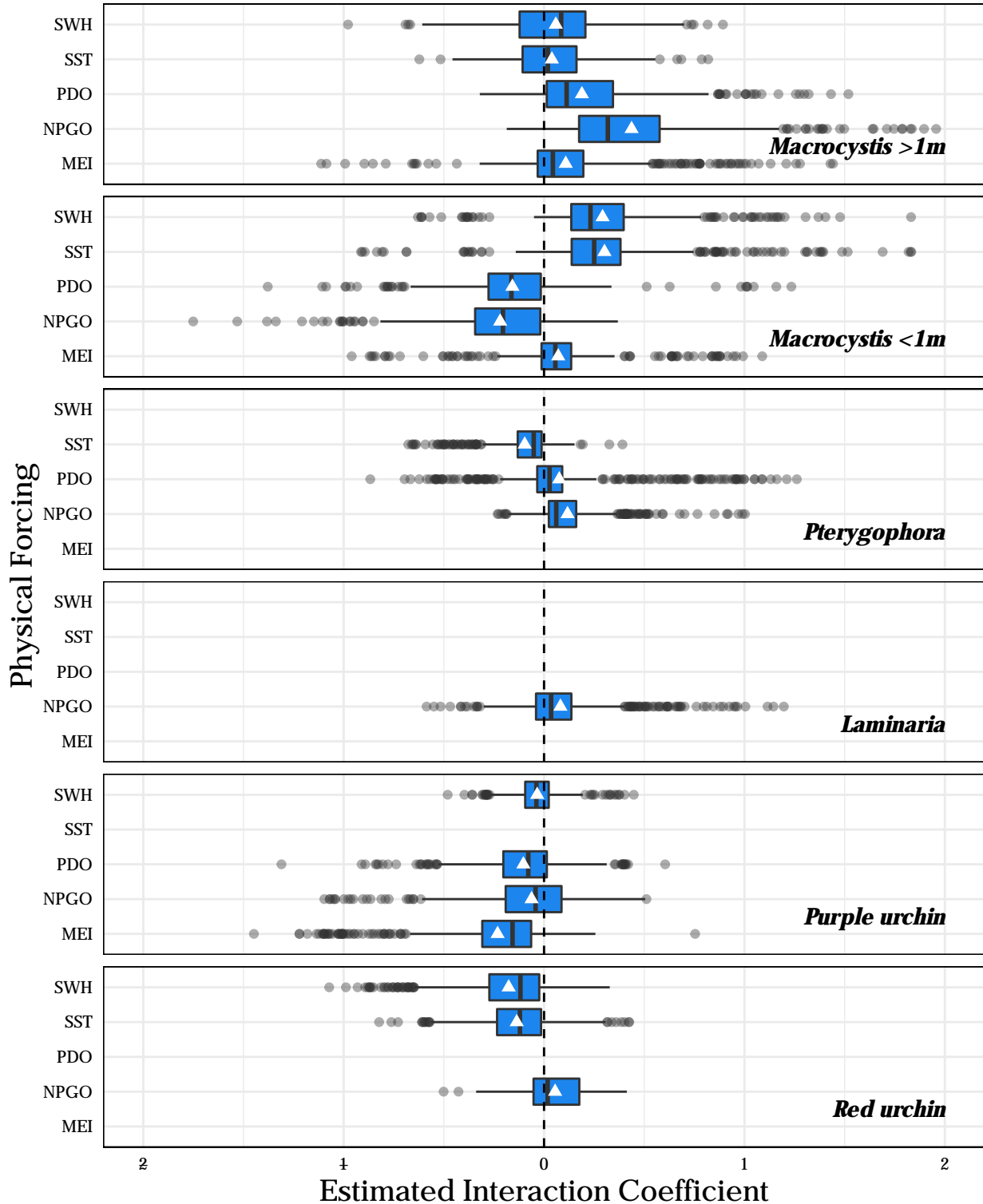
It is clear from the boxplots that fitted intra- and interspecific interactions display evidence of positive, negative, and neutral interactions. Over the range of conditions in the time series, each species variable with the exception of young *Macrocystis* has positive intraspecific effects; that is, each species' density has a positive estimated effect on itself, a combination of survivorship and new recruitment. Relative to the magnitude of other interactions, this intraspecific effect is strongest in the two urchin species.

The interactions of the urchin and algal species show evidence of herbivory (green boxes). Both red and purple urchin density have predominantly negative effect on adult and juvenile *Macrocystis*, *Laminaria*, and *Pterygophora*, effects that were consistent with our hypotheses. However, the converse effects of algal density on urchin density are generally small, and not consistently positive.

Few strong and consistent competitive interactions (red boxes) are observed in model estimates. There is evidence of competition between the two urchin species, but the interaction is small relative to other forcing factors in the urchin models, and is occasionally positive (apparent mutualism). Among the algal species, the clearest negative competitive effect is that of *Pterygophora* on adult *Macrocystis* (top panel). Other interactions are not always negative (competitive), and contrary to expectations, positive values were estimated for many interactions. *Pterygophora* has only intermittent negative effects on young *Macrocystis*, and *Pterygophora* and *Laminaria* display an apparent mutualism. Perhaps most surprisingly, *Macrocystis* does not display a consistent negative effect on *Pterygophora* or *Laminaria*, contrary to our hypothesis of *Macrocystis* competitive dominance (Dayton et al. 1999).

Multivariate Model Output: Physical Forcing

We can also investigate the effects of the physical forcing variables on the biological dynamics in a similar plot:



In this figure, each box represents the distribution of estimated effect of a physical driver (left y-axis) on the modeled species across all data for a given model. Empty rows indicate physical variables that were not included in specific species models because of a lack of a causal signal from our CCM. Abbreviations: SWH, significant wave height; SST, sea surface temperature; PDO, Pacific Decadal Oscillation; NPGO, North Pacific Gyre Oscillation; MEI, Multivariate ENSO Index.

Physical forcing variables affect the dynamics of all species in the study, to varying degrees. *Macrocystis* is the only species in the analysis that displays a significant cross-mapping signal (significant causal forcing) with all five included physical variables. The negative effects of SWH and SST on adult *Macrocystis*, and the positive effect of the NPGO, are consistent with our expectations (Bell et al. 2015). However, the PDO index has a positive effect on *Macrocystis*, contrary to expectation because in general, positive values of the PDO are associated with warmer SST and nutrient-poor conditions in the northeast Pacific. *Macrocystis* recruits, on the other hand, are positively affected by the MEI, SWH, and SST, and negatively affected by the PDO and NPGO. Together, the effects of physical forcing on *Macrocystis* suggest that conditions that are poor for survivorship of adults (higher SST, less nutrient availability, greater disturbance) may produce favorable conditions for recruitment of new sporophytes.

The physical variables are more influential drivers of *Macrocystis* than *Pterygophora* or *Laminaria* dynamics. The PDO is the only physical variable causally linked to *Laminaria* density, and it has predominantly negative but variable effect. The SWH, NPGO, MEI, and SST indices do not significantly drive *Laminaria* density. Conversely, although the PDO, NPGO, and SST were identified as causal variables for *Pterygophora* density, the magnitudes of their effects are small and inconsistent.

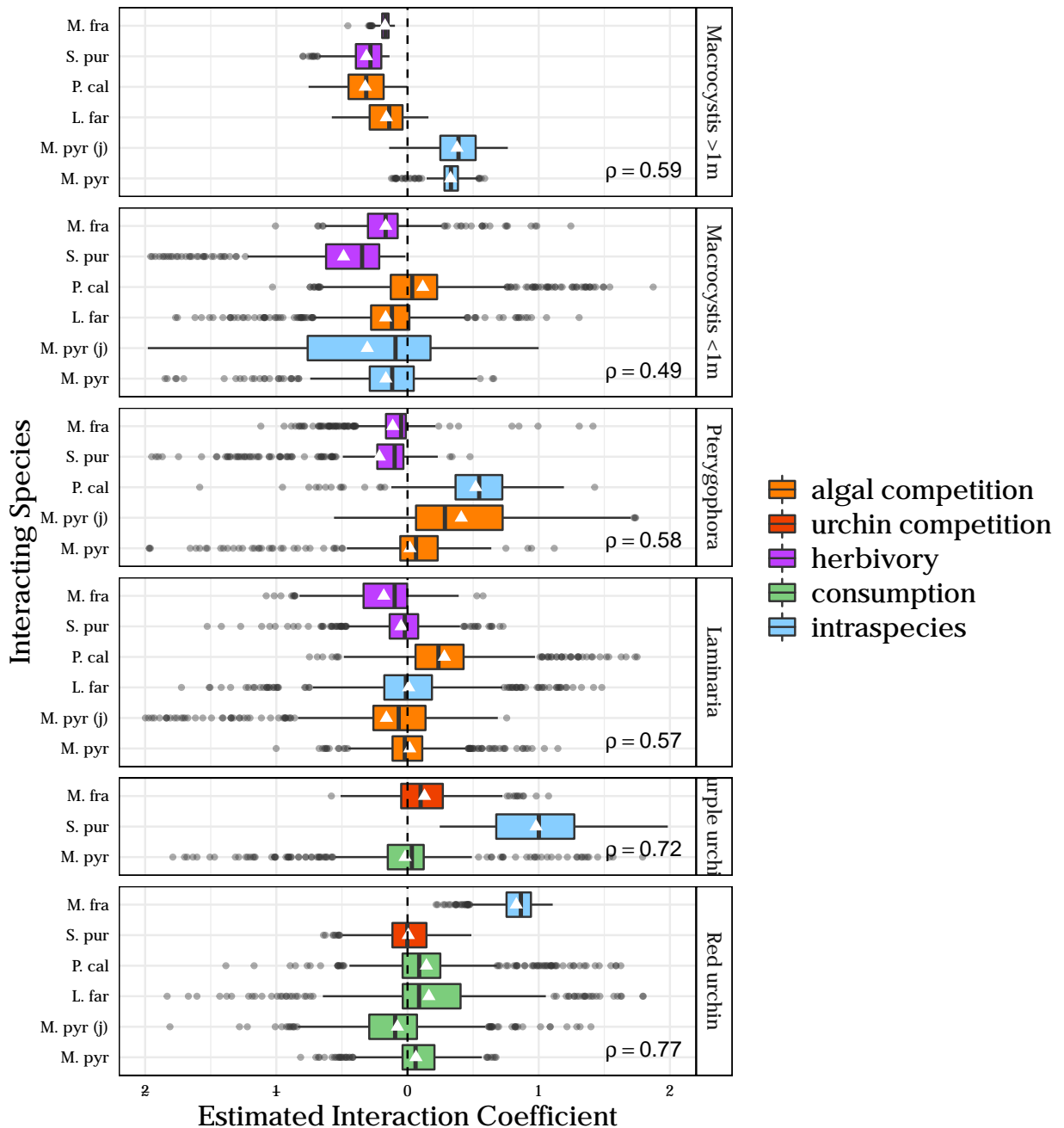
The effects of physical forcing are not limited to the algal species, although the magnitude of physical forcing effects on red urchins are small, especially compared to the effect of their own density (the intraspecific effect). For the purple urchin, the PDO, NPGO, and MEI all have negative but variable effects. For red urchin, the effects of SWH and SST are small and negative, with the PDO and NPGO have variable effects.

Physical Forcing Effect on Interactions

A major observation from the multivariate models is that many interactions between species and between species and their environments can be variable (positive or negative, depending on conditions). For the algal species especially, the combination of variable interspecific interaction strengths and occasionally strong environmental forcing effects suggests that the strength of species interactions may be driven by environmental context.

In order to observe this, we remove physical forcings and re-run the multivariate models with just the species interactions, and then look at the resulting trends through the lens of various physical forcing (to remove endogeneity). We will investigate the effect of environmental variables on interaction strength for the different interaction types (herbivory, competition, and intraspecies effects).

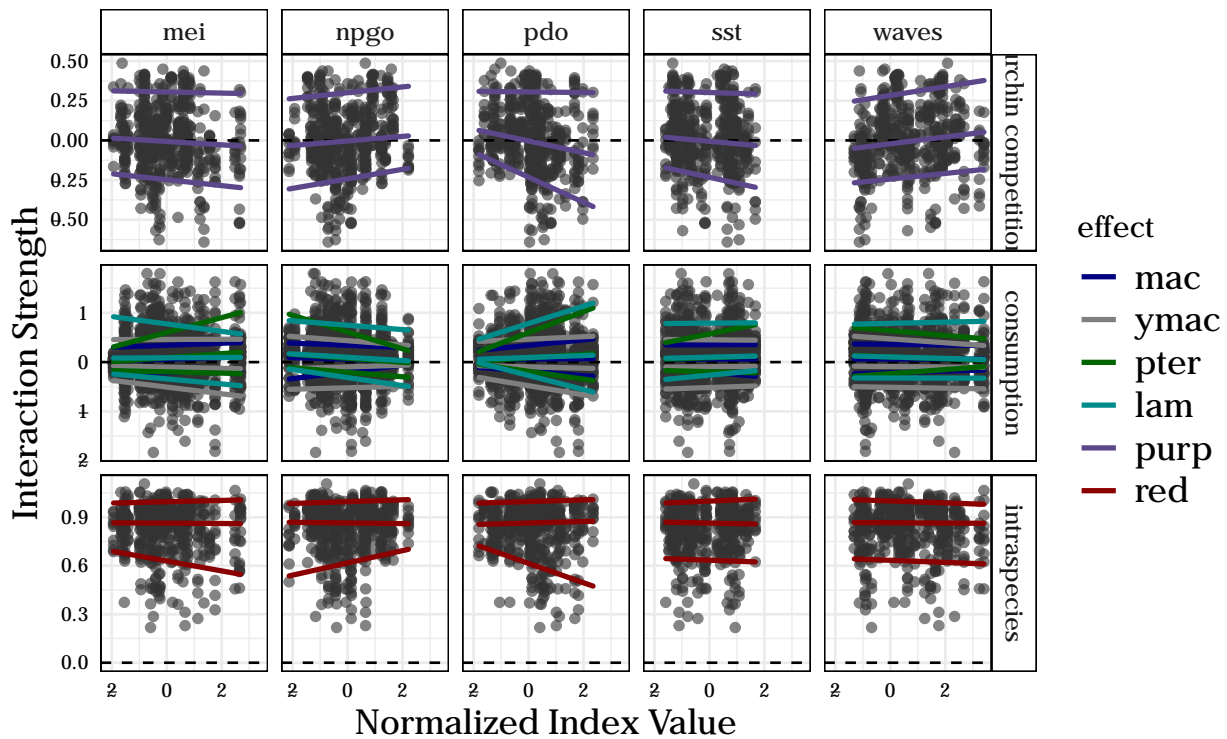
Modeled Species	Predictors	ρ	MAE
Macrocystis	Laminaria, Pterygophora, Purple urchin, Red urchin, Macrocytis <1m, Macrocytis >1m	0.587	0.501
Purple Urchin	Macrocytis >1m, Red urchin, Purple urchin	0.722	0.443
Laminaria	Macrocytis >1m, Pterygophora, Purple urchin, Red urchin, Macrocytis <1m, Laminaria	0.567	0.425
Young Macrocytis	Laminaria, Macrocytis >1m, Pterygophora, Purple urchin, Red urchin, Macrocytis <1m	0.488	0.533
Red Urchin	Laminaria, Macrocytis >1m, Pterygophora, Purple urchin, Macrocytis <1m, Red urchin	0.766	0.411
Pterygophora	Macrocytis >1m, Purple urchin, Red urchin, Macrocytis <1m, Pterygophora	0.577	0.388



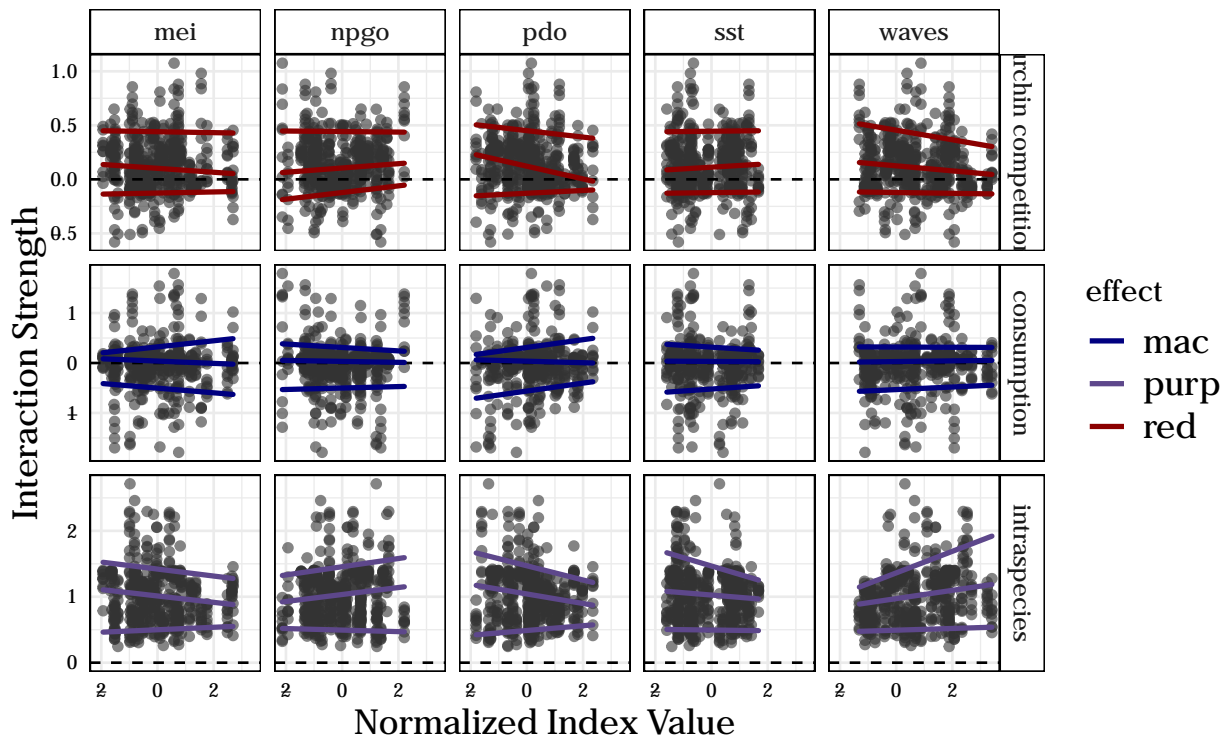
Effects on Individual Species

With 10%/90% quantile regression. Columns/x-axis indicates the level of a physical stressor, while rows and y-axis denote the type of species interaction (corresponding to the colors in the boxplots above).

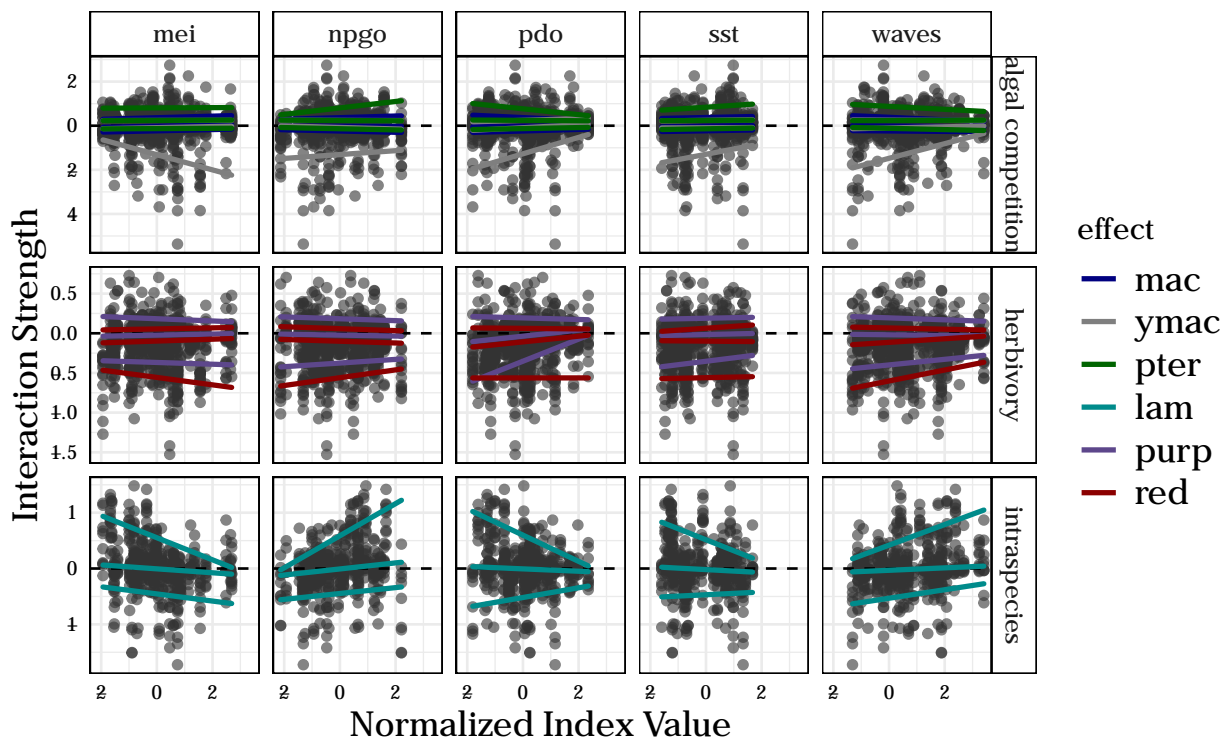
Physical forcing effect on interactions with Red urchin



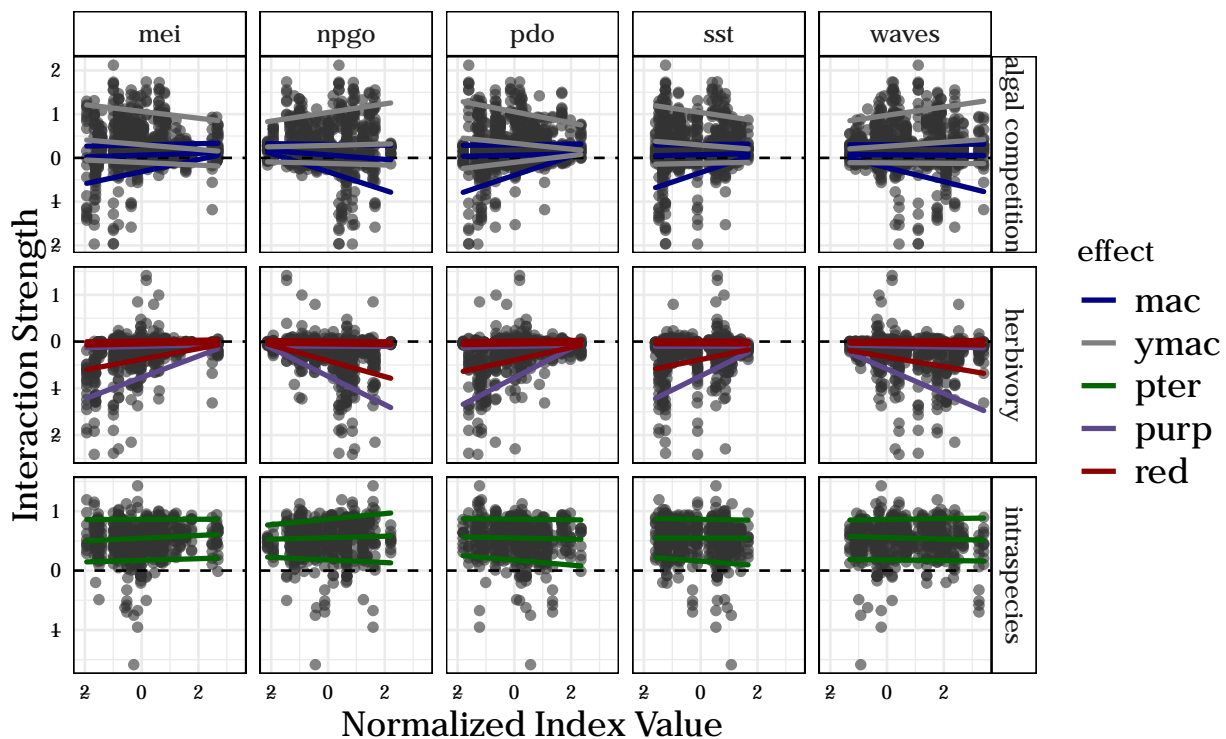
Physical forcing effect on interactions with Purple urchin



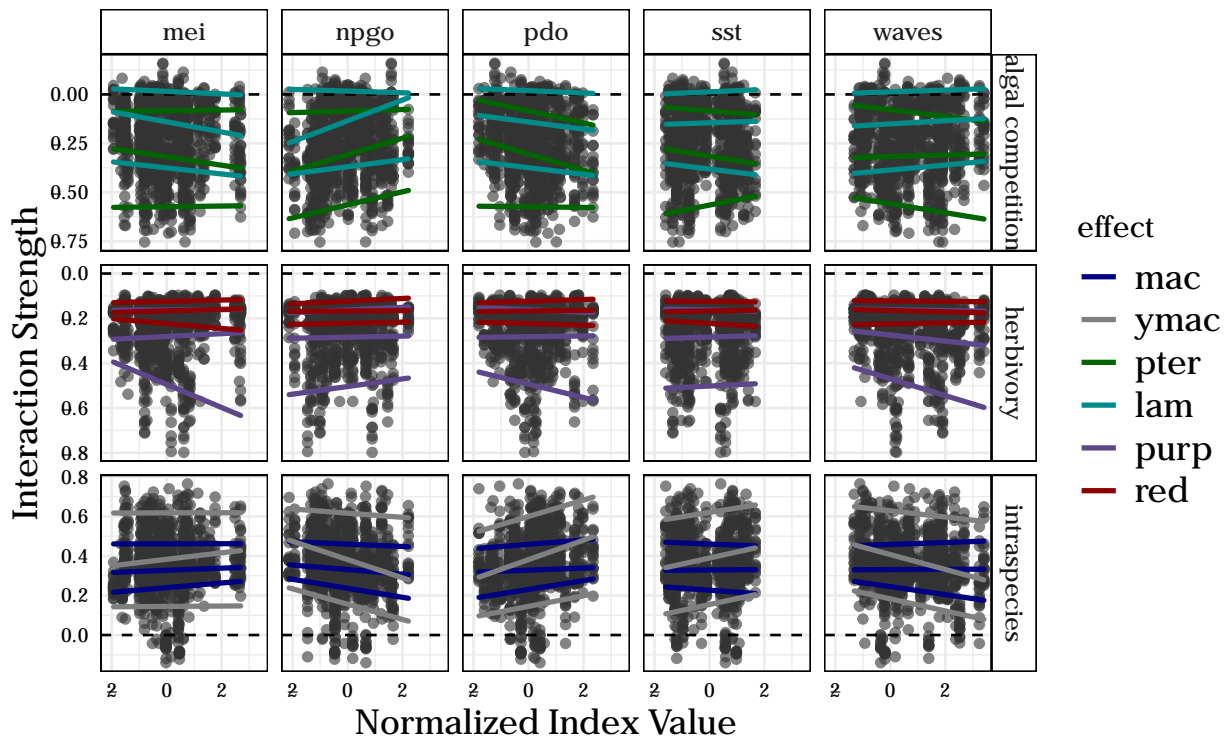
Physical forcing effect on interactions with Laminaria



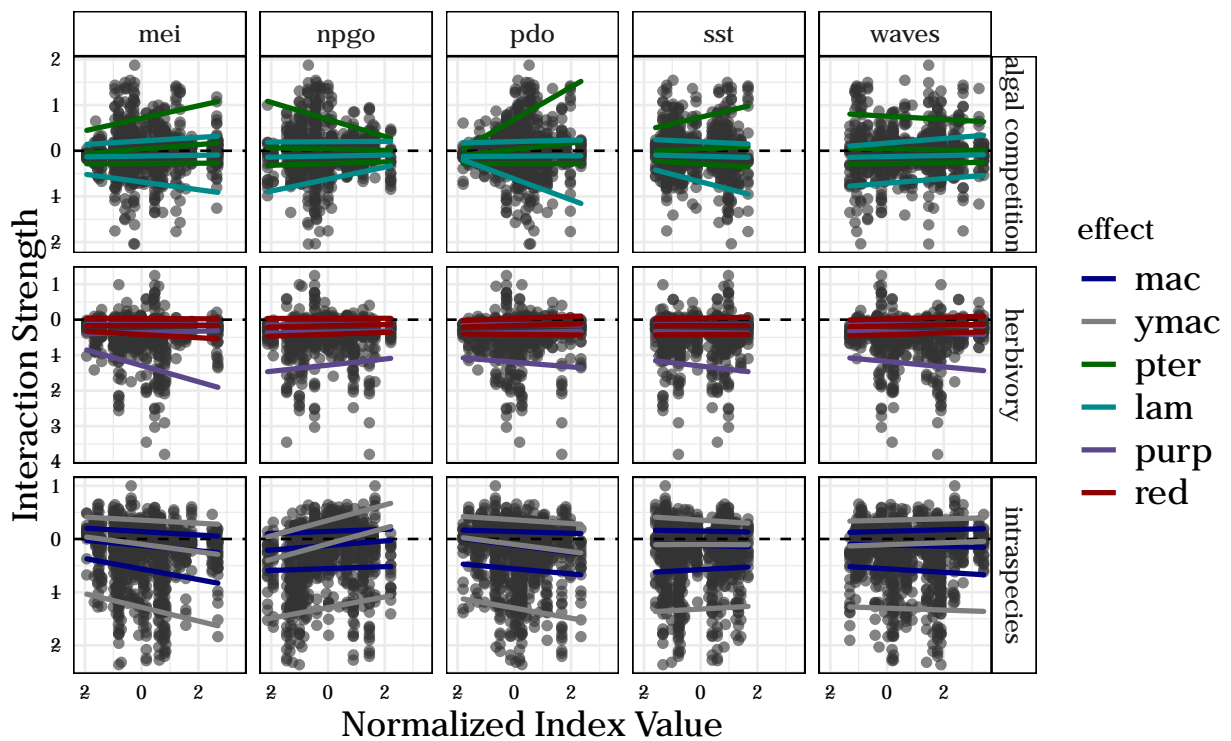
Physical forcing effect on interactions with Pterygophora



Physical forcing effect on interactions with *Macrocystis* >1m



Physical forcing effect on interactions with *Macrocystis* <1m



Here are some notable effects/trends for each species:

- *Mesocentrotus franciscanus*

- chance of competition with *Strongylocentrotus purpuratus* seems reduced under higher physical (wave) stress
 - the same (reduced competition) is marginally true for nutrient-rich conditions (higher NPGO); and the opposite for nutrient- stressed conditions (higher MEI, PDO indices)
- *Strongylocentrotus purpuratus*
 - “urchin competition” seems like a misnomer for this species; the effect of *Mesocentrotus franciscanus* on *S. purpuratus* is primarily positive across a range of physical conditions. The effect is dampened somewhat under increased wave disturbance
 - Effect of *S. purpuratus* on itself (“population growth rate” in a way) is affected by oceanographic forcing: it is slightly increased under increased NPGO values and with increased disturbance, and slightly decreased under elevated MEI, PDO, and SST.
- *Laminaria farlowii*
 - Important to note that no physical variables in this analysis showed a causal signal for *Laminaria* from CCM
 - as far as competition goes, most large, negative interactions are associated with juvenile *Macrocystis*, likely as an indicator of impending successional processes (i.e., the juvenile *Macrocystis* growing into large *Macrocystis*). This expected negative effect is reduced under elevated PDO, disturbance, and SST, which makes sense: these are conditions that classically inhibit *Macrocystis* dominance(Reed et al. 2011; Cavanaugh et al. 2011; Bell et al. 2015, Young et al. (2015)).
 - In general, *M franciscanus* has a more negative effect on *Laminaria* than does *S. purpuratus*, and that effect is not overly sensitive to physical conditions, although the negative effect is dampened somewhat under elevated disturbance
 - Physical conditions seem to strongly influence intraspecies *Laminaria* effects: the positive effect of *Laminaria* on its own density is reduced under elevated MEI, PDO, and SST, and increased under elevated NPGO and disturbance.
- *Pterygophora californica*
 - Algal effects: *Macrocystis* has a near-zero mean effect on *Pterygophora*. However, the quantile regression suggests that *Macrocystis* can have a strong negative effect on *Pterygophora* at lower relative levels of nutrient and temperature stress (high NPGO, low MEI and PDO, lower SST), and potentially after disturbance.
 - Herbivory effects on *Pterygophora* vary with physical environment. *M. franciscanus* and *S. purpuratus* have similar mean effects on *Pterygophora*, and that herbivory is sensitive to physical conditions. The effect of herbivory is strongest under elevated disturbance and NPGO, and diminished under elevated MEI, PDO, and SST.
 - Little variation in the intraspecies effect of *Pterygophora* along physical gradients.
- *Macrocystis pyrifera*
 - Because we have two variables measuring the density of different *Macrocystis* life stages, we can parse out the relative effects of physical conditions on adult vs. juvenile giant kelp.
 - Environmental stress seems to strengthen the interactions between *Laminaria* and *Pterygophora* and *Macrocystis* recruits. Under conditions of elevated MEI, SST, or PDO, or decreased NPGO, the positive effect of *Pterygophora* and the negative effect of *Laminaria* on *Macrocystis* sporophytes are both enhanced. Similar is true for the adult *Macrocystis*: interactions between the giant kelp and the other algae species are elevated under nutrient- or temperature-stressed conditions. Increased wave height (physical disturbance) seems to enhance the negative effect of *Pterygophora* on *Macrocystis* adults.
 - The effect of purple urchin on both *Macrocystis* adult and juvenile density is stronger than the red urchin effect, and more variable with changing conditions. Purple urchin herbivory as a negative influence on *Macrocystis* is enhanced with elevated disturbance, MEI, and PDO, and slightly reduced with an increase in the NPGO.
 - The strengths of intraspecies effects (effects of *Macrocystis* adults on juveniles and vice versa) are also influenced by physical conditions, but perhaps in a different way than might be expected. The positive effect of juvenile *Macrocystis* on adult *Macrocystis* seems to be **enhanced** under nutrient-stressed conditions and higher temperatures, and reduced with greater nutrient availability and increased disturbance.

Summarized effects of different physical conditions

- **Large-scale oceanographic oscillations: NPGO, MEI, and PDO**
 - Higher nutrient availability often associated with higher values of the NPGO, and lower values of the MEI and PDO.
 - High nutrient availability leads to higher urchin growth rates and reduced competition between urchin species. *Laminaria* and *Pterygophora* intraspecific effects are enhanced, while the *Macrocystis* intraspecies effect is reduced. The negative effect of herbivory is strengthened for *Pterygophora*, but reduced for *Macrocystis*. The ability of *Pterygophora* and *Laminaria* to compete with *Macrocystis* is reduced under greater nutrient availability, as evidenced by a decrease in interaction strength between the two understory species and the giant kelp, as well as an increase in the positive association of the two with each other, likely as a mutual defense against *Macrocystis* dominance.
 - The opposite of the above effects are true for nutrient-scarce conditions. High values of the MEI and PDO, and low values of the NPGO, are associated with reduced urchin growth and marginally increased urchin competition. The negative effect of herbivory is reduced for *Pterygophora*, but exacerbated for *Macrocystis*. The understory species are favored in algal competition, in that their negative effects on *Macrocystis* are strengthened, and the converse effects of *Macrocystis* on the understory are reduced. Interestingly, *Pterygophora* seems beneficial for *Macrocystis* recruitment under nutrient-stressed conditions, while *Laminaria* is inhibitory. The *Laminaria* intraspecies effect is reduced, while the intraspecies *Macrocystis* effect is enhanced.
 - The qualitative story to be told here is that under nutrient-poor conditions, a *Pterygophora* state is favored in a relative sense over a *Macrocystis* dominant state. Under nutrient-stressed conditions, *Pterygophora* is more resistant to herbivory, and more inhibitory to adult *Macrocystis*. However, *Pterygophora* is beneficial for *Macrocystis* recruitment, while *Laminaria* inhibits *Macrocystis* recruitment under nutrient stressed conditions. When conditions are “better” (more nutrients), *Macrocystis* gains. It becomes more able to withstand herbivory, less sensitive to *Pterygophora* or *Laminaria* presence, and more inhibitory to *Pterygophora*.
- **Temperature**
 - Elevated SST has similar effects to nutrient stress (elevated MEI and PDO, and reduced NPGO), which makes sense: In Southern California, elevated SST is associated with reduced nutrient availability(Zimmerman and Kremer 1984,Bell et al. (2015)). Similar effects as described above for nutrient stress hold for elevated temperature.
- **Physical disturbance**
 - Higher max wave heights was our proxy for physical stress/disturbance.
 - Higher physical disturbance levels results in reduced interaction strength between the urchin species.
 - *Pterygophora*’s competitive ability is enhanced with increased disturbance(Dayton et al. 1999), evidenced by an increase in the negative effect of *Pterygophora* on adult *Macrocystis*.
 - *Pterygophora* and *Macrocystis* are both subject to a greater negative effect of herbivory under increased disturbance.
 - *Laminaria* benefits as well. The negative effects of herbivory and algal competition are reduced with increased disturbance, and its intraspecies effect is strengthened.
 - The positive effect of juvenile on adult *Macrocystis* is reduced with increased physical stress.

References

- Bell, Tom W., Kyle C. Cavanova, Daniel C. Reed, and David A. Siegel. 2015. “Geographical variability in the controls of giant kelp biomass dynamics.” *Journal of Biogeography* 42 (10): 2010–21. doi:10.1111/jbi.12550.
- Cavanaugh, Kyle C., David A. Siegel, Daniel C. Reed, and Philip E. Dennison. 2011. “Environmental controls of giant-kelp biomass in the Santa Barbara Channel, California.” *Marine Ecology Progress Series* 429: 1–17. doi:10.3354/meps09141.
- Chang, Chun Wei, Masayuki Ushio, and Chih hao Hsieh. 2017. “Empirical dynamic modeling for beginners.”

Ecological Research. Springer Japan, 1–12. doi:10.1007/s11284-017-1469-9.

Clark, A. T., Hao Ye, F. Isbell, E. R. Deyle, J. Cowles, D. Tilman, and George Sugihara. 2015. “Spatial convergent cross mapping to detect causal relationships from short time series.” *Ecology* 96 (5): 1174–81.

Dayton, Paul K. 1985. “The Structure and Regulation of Some South American Kelp Communities.” *Ecological Monographs* 55 (4): 447–68.

Dayton, Paul K, Mia J. Tegner, Peter B. Edwards, and Kristin L. Riser. 1999. “Temporal and spatial scales of kelp demography: the role of oceanographic climate.” *Ecological Monographs* 69 (2): 219–50. doi:10.1890/0012-9615(1999)069[0219:TASSOK]2.0.CO;2.

Deyle, Ethan R, Michael Fogarty, Chih-hao Hsieh, Les Kaufman, Alec D Maccall, and Stephan B Munch. 2013. “Predicting climate effects on Pacific sardine.” *Proceedings of the National Academy of Sciences of the United States of America* 110 (16): 6430–5. doi:10.1073/pnas.1215506110/-/DCSupplemental.www.pnas.org/cgi/doi/10.1073/pnas.1215506110.

Deyle, Ethan R., Robert M. May, Stephan B. Munch, and George Sugihara. 2016. “Tracking and forecasting ecosystem interactions in real time.” *Proceedings of the Royal Society B: Biological Sciences* 283 (1822): 20152258. doi:10.1098/rspb.2015.2258.

Di Lorenzo, E., N. Schneider, K. M. Cobb, P. J S Franks, K. Chhak, A. J. Miller, J. C. McWilliams, et al. 2008. “North Pacific Gyre Oscillation links ocean climate and ecosystem change.” *Geophysical Research Letters* 35 (8): 2–7. doi:10.1029/2007GL032838.

Graham, Michael H, Julio A Vásquez, and Alejandro H Buschmann. 2007. “Global Ecology of the Giant Kelp *Macrocystis* : From Ecotypes To Ecosystems.” *Oceanography and Marine Biology* 45: 39–88. <http://scholar.google.com/scholar?hl=en&btnG=Search&q=intitle:Global+ecology+of+the+giant+kelp+Macrocystis:+>

Hsieh, Chih-hao, Christian Anderson, and George Sugihara. 2008. “Extending nonlinear analysis to short ecological time series.” *The American Naturalist* 171 (1): 71–80. doi:10.1086/524202.

Reed, Daniel C., Andrew Rassweiler, Mark H. Carr, Kyle C. Cavannaugh, Daniel P. Malone, and David A. Siegel. 2011. “Wave disturbance overwhelms top-down and bottom-up control of primary production in California kelp forests.” *Ecology* 92 (11): 2108–16. doi:10.1890/11-0377.1.

Sugihara, George. 1994. “Nonlinear forecasting for the classification of natural time series.” *Philosophical Transactions of the Royal Society of London Series A-Mathematical Physical and Engineering Sciences* 348: 477–95.

Sugihara, George, Robert May, Hao Ye, Chih-hao Hsieh, Ethan Deyle, Michael Fogarty, and Stephan Munch. 2012. “Detecting causality in complex ecosystems.” *Science* 338 (6106): 496–500. doi:10.1126/science.1227079.

Ye, Hao, Ethan R Deyle, Luis J Gilarranz, and George Sugihara. 2015. “Distinguishing time-delayed causal interactions using convergent cross mapping.” *Scientific Reports* 5. Nature Publishing Group: 14750. doi:10.1038/srep14750.

Young, Mary Alida, Kyle C. Cavannaugh, Tom W. Bell, Peter T. Raimondi, Christopher A. Edwards, Patrick T. Drake, Li Erikson, and Curt Storlazzi. 2015. “Environmental controls on spatial patterns in the long-term persistence of giant kelp in central California.” *Ecology* 86 (1): 45–60. doi:10.1890/15-0267.1.

Zimmerman, Richard C., and James N. Kremer. 1984. “Episodic nutrient supply to a kelp forest ecosystem in Southern California.” *Journal of Marine Research* 42 (3): 591–604. doi:10.1357/002224084788506031.